

# Data-driven Simulation Framework for Expressive Piano Playing by Anthropomorphic Hand with Variable Passive Properties

Huijiang Wang<sup>1</sup>, Toby Howison<sup>1</sup>, Josie Hughes<sup>2</sup>, Arsen Abdulali<sup>1</sup> and Fumiya Iida<sup>1</sup>

**Abstract**—The expressive piano playing generally requires a delicate control over the keystroke by considering passive dynamics of the hand and piano keyboard. It becomes even more challenging when the passive properties change during the performance. In this paper, we develop a framework for expressive piano playing that simulates the interaction between a soft anthropomorphic hand with variable passive properties and a piano keyboard. The passive dynamics of each system component in our framework are identified using the data collected during real piano playing, which in turn, helps to reduce the sim-to-real gap. To evaluate the proposed framework, we have designed and fabricated a three-fingered soft-rigid hybrid hand system with variable stiffness in each finger, enabling diverse compliant behaviors for piano key pressing. The results show that our proposed simulator achieves less than 5% error rate in coordination with real-world piano playing.

## I. INTRODUCTION

Music acts as a barrier-free language that allows for communication and the sharing of emotions. Many musical instruments require manipulation capabilities that are subtle and dexterous to achieve the artful creation of sound. With advances in robotic capabilities, there is increasing interest in developing robots that can perform music in a human-like way as it provides a benchmark for assessing the performance of robots [1], [2]. Piano playing is another challenge that is particularly interesting for robotics as it requires extreme dexterity of the hand and also exploits the hand’s passive properties to achieve different styles of playing. Although piano playing robots exist, many approaches, however, are limited in their expressiveness and their ability to achieve dynamics and artistry that is close to that of human playing [3].

The research on robotic piano playing started from the 1980s [4] and has been constantly evolving in terms of the actuation methods [5], [6] and controller designs [7]. Recent research on controller design has been focusing on expressive piano playing that enables robots to play a music piece in various styles. For instance, Gaussian Process (GP) [8] and Recurrent Neural Networks (RNN) [9] have been utilized to incorporate different styles into a keystroke controller. The robotic hand used along with the most recent controller designs was rigid to avoid modeling complex passive dynamics of a soft hand. Passive dynamics, on the



Fig. 1. Anthropomorphic three-fingered robot hand with variable stiffness joints and its simulated replication.

other hand, have been proven to be beneficial in robotic piano playing. For instance, in [10], a passive anthropomorphic piano hand was fabricated using multi-material 3D printing allowing the piano plying with only wrist actuation. However, modeling various playing styles for an anthropomorphic hand that changes passive properties still remains open to research, e.g., stiffness-tuneable robot hands [11]–[13], variable stiffness phalange [14], and particle jamming hand [15]. Additionally, it would also be advantageous if a single set of piano playing styles is applied to different anthropomorphic hands with diverse mechanical properties.

In this work, we proposed a novel simulation-based framework incorporating modeling contact dynamics of the keystroke, passive dynamics of the anthropomorphic hands, and expressive piano styles. The main focus of the simulator is to reduce the so called ‘sim-to-real’ gap, which allows training and deploying complex black-box controllers, e.g., deep [9] and reinforcement learning [16]. The framework reduces the gap by comparing generated and measured Musical Instrument Digital Interface (MIDI) signals, rather than focusing on the physical interaction. This enables the robot closer to reproduce the style of the pianist by considering the passive dynamics of the hand. To evaluate the proposed framework, we fabricated the anthropomorphic hand with variable stiffness. We identified models of passive dynamics for three different levels of stiffness. The experimental results show that the framework can reproduce piano playing styles with a negligible ‘sim-to-real’ gap. As such this paper makes a number of contributions:

- Development of the framework for modeling interaction between piano keyboard and soft hand.
- Development of the identification method that narrows ‘sim-to-real’ gap and allows deploying the controller to real robot-piano interaction.
- Fabrication of a three-finger anthropomorphic hand with

<sup>1</sup>Bio-Inspired Robotics Lab, Department of Engineering, University of Cambridge, CB2 1PZ, UK. {hw567, th533, aa2335, fi224}@cam.ac.uk

<sup>2</sup>CREATE-LAB, School of Engineering, École Polytechnique Fédérale de Lausanne, CH-1015 Lausanne, Switzerland. josie.hughes@epfl.ch

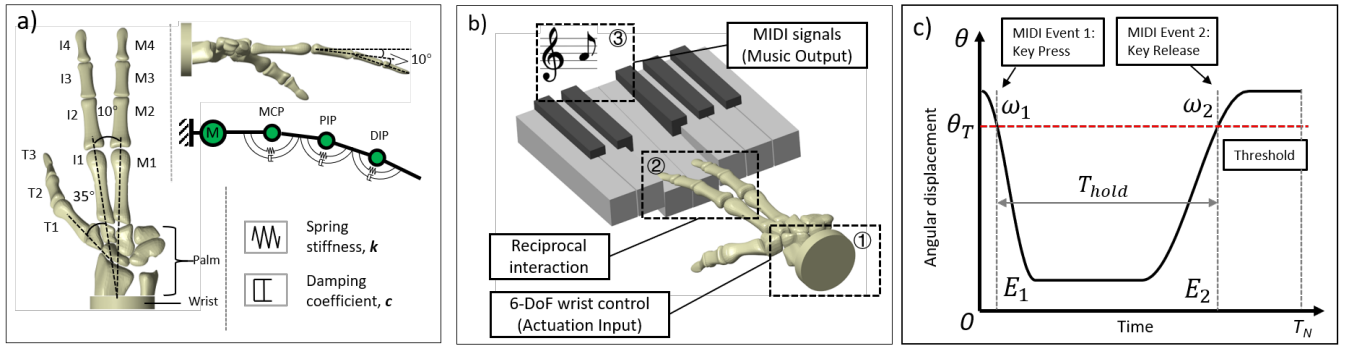


Fig. 2. Different components of the simulation platform. (a) The anthropomorphic hand consists of 13 objects placed as a natural bending pose. The revolute joints between two phalanges are characterized by spring stiffness and damping coefficient. (b) An octave starting from note C is simulated with 7 white keys and 5 black keys. Angular displacement of the key can be detected as a result of the finger-key contact. (c) Musical phrase produced from a single-note key-strike action is parameterized by two MIDI events. A triggering threshold is used to determine the key-press and key-release motions.

variable-stiffness based-on particle jamming.

## II. SIMULATOR DESIGN

In this section, we introduce the design of the simulator that was developed using Simscape Multibody Simulation environment. The simulation environment is composed of three parts. First, the CAD model of the anthropomorphic hand was imported and the deformation model between each phalange was implemented. Second, we constructed the piano keyboard with seven keys that can produce a complete octave, i.e., 7 notes in the diatonic scale. Finally, we developed the model of finger-key interaction, where the musical phrases were parameterized as MIDI signals corresponding to various mechanical interactions in the simulation.

### A. Anthropomorphic Hand

The three-fingered hand is modelled as 13 3D objects i.e., 1 object for the palm, 3 bones for the thumb, and 4 phalanges for the other two fingers. As illustrated in the of Fig. 2(a), each phalange of three fingers were enumerated starting from the palm, e.g., the phalanges of the thumb was labeled as T1, T2 and T3. To simulate a natural piano keystroke, we empirically set the angles between the thumb and index fingers to 35 degrees. The angle between index and middle fingers were set to 10 degrees (see Fig. 2(a)). Moreover, except for the index and middle fingertips (I4 and M4) that are aligned with their third bones, all the phalanges were assembled with a 10 degrees offset with respect to the adjacent bones, as shown in Fig. 2(a). The density of the imported geometric objects was set to 1900 kg/m<sup>3</sup> to minimize the gap between the simulated and real human bones [17].

A kinematic model of the linking joints between phalanges was also created in the simulation. The interphalangeal (IP) joints (see Fig. 3) were defined as one-DoF revolute joint to allow only the flexion-extension motions while the MCP joints were represented by universal joint with 2 DoFs to also allow abduction-adduction motions between fingers. To represent the relative motion between the bones, each revolute joint was modelled as a rotational spring-damper

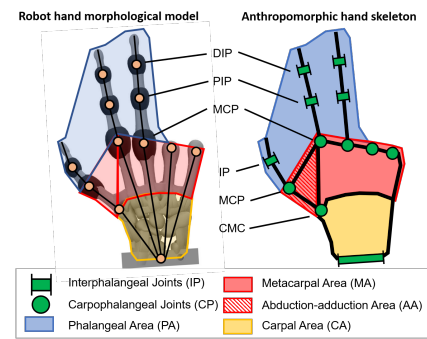


Fig. 3. Anthropomorphic hand skeleton and its morphological model

system where the the kinematic motion between two adjacent phalanges was defined as

$$J\ddot{\alpha} + c\dot{\alpha} + k\alpha = 0 \quad (1)$$

where  $\alpha$ ,  $\dot{\alpha}$  and  $\ddot{\alpha}$  denote the angular displacement, velocity and acceleration, respectively. The momentum of inertia of the dynamic phalange was calculated by  $J = \sum_i \Delta m_i r_i^2$ , where  $\Delta m$  and  $r$  denote the  $i$ th unit mass element and distance to the revolute axis.  $k$  and  $c$  denote the spring stiffness and damping coefficient, respectively.

### B. Piano Environment

We modelled 12 chromatic notes of the piano including 7 white keys plus 5 black keys, with the segment starting from Note C. Each key was independent and modelled as a cuboid with a density of wood. Each piano key was constrained on the end by a revolute joint with equilibrium position at 0 degrees, allowing only downward rotation.

The keystroke action was represented as the collision between the fingertip and the piano key, with measurement of the normal and frictional forces added at this point to allow for dynamic analysis of the finger-key interactions.

### C. Musical Signal Parameterization

To simulate the music for each keystroke, we defined a triggering angular displacement  $\theta_T$ , i.e., is a threshold

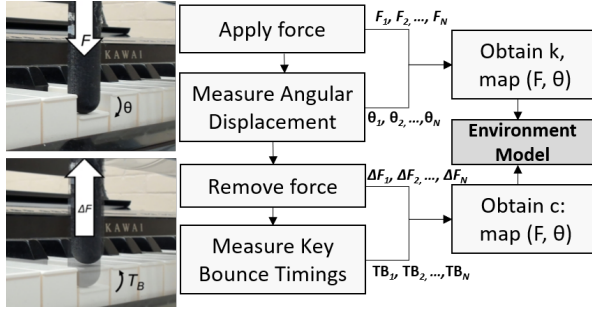


Fig. 4. System identification of the spring-damping system of the piano notes.

when the key produces an acoustic output. When the key displacement reaches this threshold level, a MIDI event is recorded and corresponding keystroke velocity is recorded. When the key is released, another MIDI message with the timestamp is captured. (see Fig. 2(c)). These two MIDI messages characterize a key press.

$$\begin{cases} V_{pre} = r \cdot \omega_1, \\ V_{rel} = r \cdot \omega_2, \\ T_{hold} = E_2 - E_1, \\ T_{idle} = T_N - T_{hold}. \end{cases} \quad (2)$$

where  $\omega$  and  $T_{hold}$  denote the angular velocity and duration of the keystroke,  $r$  is the distance from the axle of revolution to the contact position, and  $T_N$  denotes the note length. These variables were sensed from the simulator and used to calculate four parameters characterizing the quality of the produced music. In Eq. 2,  $V_{pre}$  and  $V_{rel}$  denote the velocities when the key was pressed and released. For practical musical purpose, the velocity is usually normalized in the range between 0-127, which also correlates with the force of the keystroke. The length of actual keystroke action ( $T_{hold}$ ) is a crucial parameter governing the articulation, while  $T_{idle}$  is the period during which the key is not triggered and waiting for the next keystroke.

### III. MODEL IDENTIFICATION

In this section, we focus on model identification of passive dynamics of the antropomorphic hand and piano keyboard by employing a Bayesian optimization framework. The optimized parameters then were used in stiffness modulation in simulator, as well as was later applied in the experiment (see Sec. IV) via the control of vacuum pressure in granular jamming.

#### A. Keystroke Model Identifications

The internal mechanical parameters  $k$  and  $c$  of the revolute joint were identified using the data collected from the real piano keyboard. The data collection process is depicted in Fig. 4. By applying a load to the piano keys ( $F$  sequence), the corresponding angular displacements ( $\theta$  sequence) were recorded to identify the stiffness component. Likewise, we obtained the damping coefficient by abruptly removing the applied load. The objective of the optimization is to minimize

errors between simulated and real angular displacements, as well as bounce time before and after the removal of the load.

#### B. Passive Parameters Optimization

Given the user-defined MIDI sample, the goal of the model is to reproduce the piano playing scenario by optimizing passive parameters. The reference MIDI signals can be either collected from experimentation or generated by a computer composer. As mentioned in section II-A, the spring stiffness  $k$  is the pivotal argument that determines the compliant behaviors of fingers. In the simulation, we aimed to optimize the spring stiffness to obtain the desired MIDI signals with given sheet music and fixed wrist control. A Bayesian optimization problem is defined as follows

$$\begin{aligned} & \arg \min_{k \in S} \lambda_1 f_d(k) + \lambda_2 f_a(k). \\ & \lambda_1, \lambda_2 \in [0, 1] \\ & \lambda_1 + \lambda_2 = 0 \end{aligned} \quad (3)$$

where

$$\begin{cases} f_d(k) = \|V_{pre} - V_{pre}^*\| + \|V_{rel} - V_{rel}^*\|, \\ f_a(k) = \|T_{hold} - T_{hold}^*\| + \|T_{idle} - T_{idle}^*\|. \end{cases} \quad (4)$$

The objective of the optimization is minimization of the error between the MIDI output from simulation and the reference signal. In Eq. 3,  $S$  denotes the design space of the stiffness while  $f_d$  and  $f_a$  characterize the errors in dynamics (governing the loudness) and articulation (determining the rhythm) of the produced musical phrases. Weight coefficient  $\lambda$  was introduced to adjust the preference for these two crucial playing patterns. In Eq. 4, the arguments with asterisks represent the reference values. To evaluate the performance of the simulator, the error metric was introduced as

$$\begin{aligned} Err = & \frac{\lambda_1}{2} \left( \frac{|V_{pre} - V_{pre}^*|}{V_{pre}^*} + \frac{|V_{rel} - V_{rel}^*|}{V_{rel}^*} \right) \\ & + \frac{\lambda_2}{2} \left( \frac{|T_{hold} - T_{hold}^*|}{T_{hold}^*} + \frac{|T_{idle} - T_{idle}^*|}{T_{idle}^*} \right). \end{aligned} \quad (5)$$

The workflow of the optimization is illustrated in Fig. 5. Firstly, an initial stiffness argument was used in the simulator to perform key-hitting actions. Subsequently, the simulator determined whether the corresponding piano note is triggered by inspecting the contact forces among blocks. If a keystroke action was detected, two MIDI events will be recorded and parameters (see Eq. 2) reflecting the quality of the produced musical phrase would be obtained. Otherwise a penalty was introduced. Finally, if the stop criteria were violated, an updated stiffness parameter was then sent back to the simulator and another round of iteration would be carried out until the framework output optimized passive parameters and the corresponding MIDI signals.

#### C. Real-to-Sim Transfer

With the given optimization framework above, the optimal stiffness parameter can be obtained and consequently the simulation-produced MIDI signals can track the user-defined

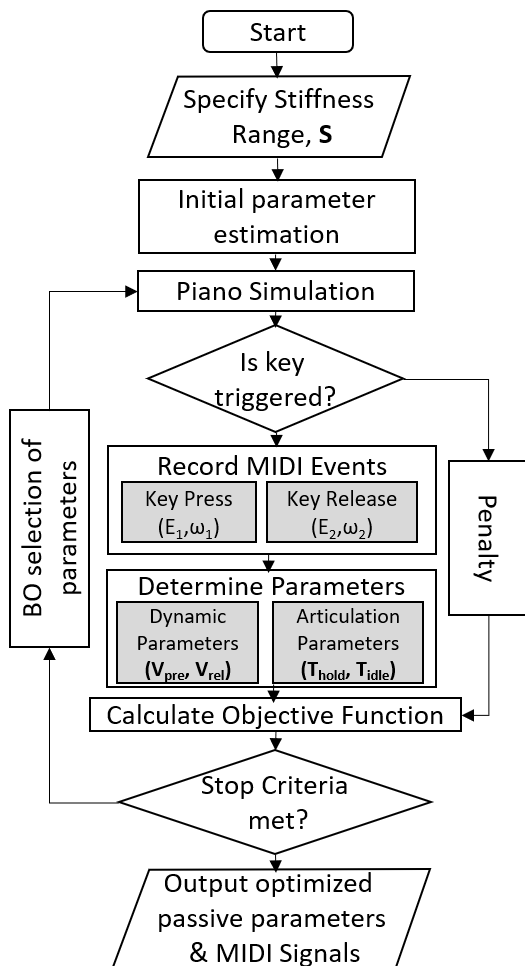


Fig. 5. Flowchart of the passive parameter optimization.

MIDI input with high accuracy. The simulator and the robot platform can be synchronized in terms of the wrist actuation, finger-key interaction, MIDI events triggering and musical phrases production. For single-note key-press actions, we fixed the wrist control as hybrid sinusoidal up-down displacement[8]. With the sample music represented by 4-dimensional MIDI signals, we initialized the real and virtual wrist to the same position and orientation. This will lead to similar hand-piano contacts since the simulation is a replication of the real robot platform. The simulator produced the MIDI output according to the angular displacement and the triggering threshold while the actual MIDI signals was collected from the digital piano. The stiffness level was switched from soft to hard by varying vacuum pressure. This allows producing various passive behaviors when interacting with the piano, leading to different groups of MIDI signals. The optimization would then proceed and this would result in the acoustic production in simulation akin to the original sheet music.

#### IV. EXPERIMENTAL SETUP

In this section, we explain fabrication process and the hardware that we used for the piano playing. The anthropo-

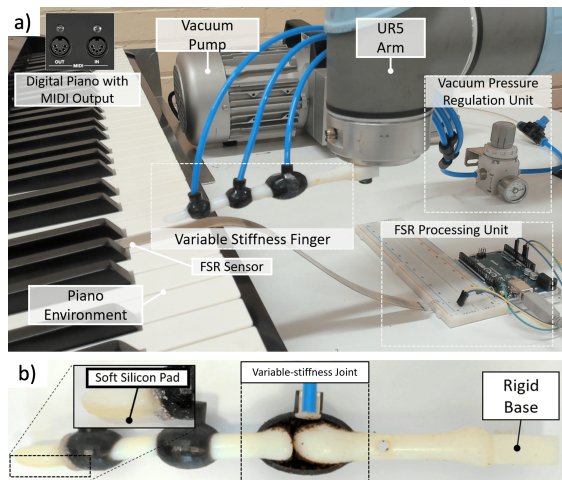


Fig. 6. The experimental setup. (a) Key-press actions are produced between the anthropomorphic finger and the piano keys. (b) The soft finger comprises of three variable-stiffness joints, where rubber cage with particles inside the chamber forms the main structure, while sealant and filter mesh are used to eliminate air leakage and prevent the coffee powder from entering the vacuum tube.

morphic hand was printed using a *Stratasys Connex 500* 3D printer. Bones of the hand was printed using rigid material (RGD450), whereas surrounding ligaments linking bones at joints were printed using Agilus30Black, a rubber like-material. After printing, each encapsulated joint is filled with jamming particles (as shown in Fig. 6(b)). The air outlet with a mesh filter to control the jamming effects was connected to the jamming chamber. Ground coffee was chosen as the granular matter for its ease of access and swift transition in stiffness. A soft silicon pad (Ecoflex 10, Smooth-on Inc.) was attached to the fingertip to increase the contact area and provide additional compliance to the finger tip. The wrist of the 3D printed anthropomorphic hand was mounted on a 6-DoF UR5 robot arm. The variable stiffness fingers were powered by a vacuum pump and controlled by regulators (SMC IRV10-N07). The vacuum pressure varied from 0 to up to -100 KPa relative to atmospheric pressure. A Kawai ES8 digital piano was used for the experiments. It supported both the input and output of MIDI signals, with the same format at the simulator. A Force Sensing Resistor (FSR) was added to a piano key to obtain a ground truth of the force applied in the real world. The FSR was calibrated to allow the force in Newtons to be reported by a microcontroller.

#### V. RESULTS

To evaluate the proposed framework, we performed two experiments. First, three piano playing styles were simulated to validate the effectiveness of the established simulation platform. Second, to illustrate the the effective of the proposed framework in terms of reduction of the 'sim-to-real' gap, we ran optimization routines that we presented in Sec.III-B.

##### A. Validation of the Simulator

To validate the effectiveness of the simulation platform, we exploited the simulator to play three musical phrases.

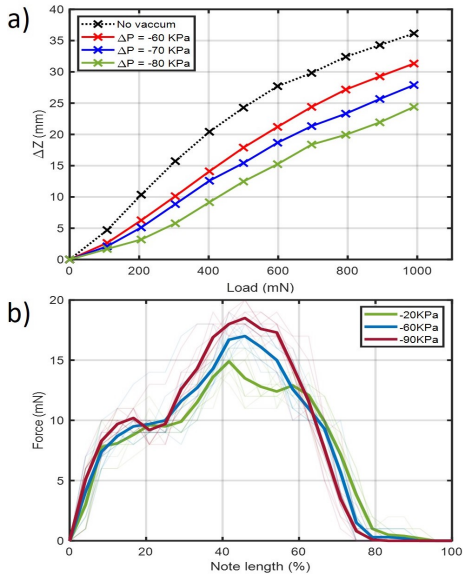


Fig. 7. Demonstration of stiffness adjustability. (a) Vertical displacement of fingertip vs. load, (b) Finger-key contact force within single-note key-press action and the corresponding.

Primarily, single-note key-press was simulated with varying stiffness parameters ( $k$ ). While the angular displacement for all cases demonstrated similar variations, the maximum finger-note contact force rose from 3.71 mN to 14.6 mN as  $k$  switched from 0.05 N\*m/deg to 2 N\*m/deg. This is in line with the force-stiffness variation pattern in real experiment (Fig.7b). The transient bulges occurred between 1-2s resulted from the fact that the piano note reached its rotational limitation. In addition, a glissando was played by enabling the thumb to slide on the whole octave. Fig.8(b) depicted the MIDI information associated with each piano note. The intermediate five notes demonstrated stable and similar inter-note shifts while the imparities on Note C and B were due to the extra subtle behaviors in glissando initiation and termination. Finally, a case study of two-note hand stretch was implemented to show the capability of staccato control. Note E was pressed by the thumb while note G-sharp by the middle finger. Each note was separately hitted twice but the second hit was via a swifter wrist control. In Fig.8(c), different from Note G-sharp, the Note E was successfully triggered without touching the rotational limitation. A shorter duration of key-press was witnessed in the fast-press trial, which means that the slow-to-fast staccato style can be simulated. With an external MIDI device (Kawai ES8), the auditory sound generated by our simulator was played and the production of three musical phrases was presented in Supplementary Videos. It can be validated that the simulator is capable of mimicking the mechanical hand-piano interaction and producing actual acoustic MIDI output.

### B. Robot-simulation Coordination

With a fixed vacuum pressure applied to the anthropomorphic hand, we performed two-note key presses in robot platform. The resultant MIDI signals were collected and used as the reference values. A Bayesian optimization was then

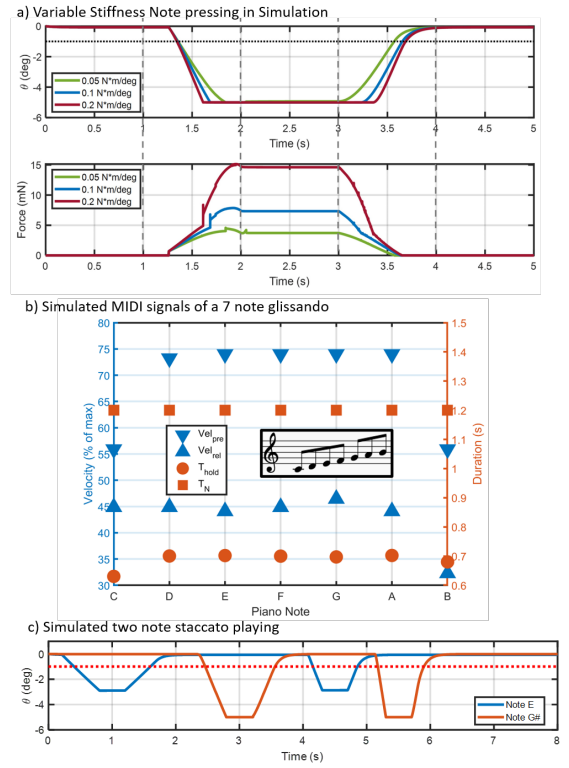


Fig. 8. Three musical phrases are played using the simulator: (a) Single-note key-press with varying stiffness coefficients and the corresponding contact forces; (b) MIDI signals of glissando imitation; (c) Angular displacement of staccato two-note playing style.

implemented to compute the optimal stiffness parameters. The weight coefficients  $\lambda_1$  and  $\lambda_2$  in Eq.4 were set to 0.8 and 0.2, respectively. The optimization was carried out with 30 iterations and the total length of one individual key strike was 2.5s. It can be seen from Fig.9 that the simulation achieved good replication of the musical phrases in terms of key-press and key-release velocities. However, with the optimized stiffness parameter ( $k$ ), there was an obvious deviation between the simulator-produced  $T_{hold}$  and that from the ground truth. This was due to that the objective function prioritized the velocities with a higher weight coefficient. Based on the definition in Eq.5, the error rate of the simulator was computed and the result showed that our simulator achieved overall 4.41% error rate in a typical two-note piano playing, signifying that a closed robot-simulator coordination was approached.

## VI. DISCUSSION & CONCLUSION

We presented a simulation platform to achieve a near-exact replication of the piano playing scenario, within which the mechanical humanoid geometries, piano environment, and meaningful music representations were imitated. The high-fidelity simulator can reproduce the passive hand-piano interactions and generate multiple musical phrases. An optimization method that utilizes the produced music as a mean to compute the passive parameters was presented to make it possible to traverse the design space for the soft hand.

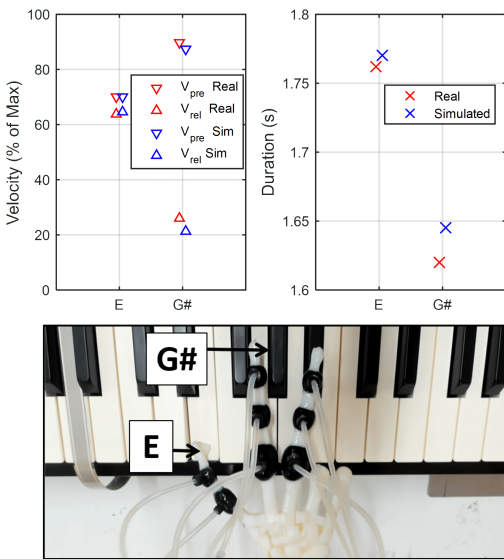


Fig. 9. Comparison of MIDI velocity signals (top-left) and holding time (top-right) for the two-note playing between the simulation and ground truth.

The simulator accompanying the optimization enabled the closed gap between simulation and real world experiment for complex multi-body challenge of piano simulation.

There are various directions to improve current work in future research. First, the actuation of individual fingers would enhance the reachability of the fingertips, which would enable the robot hand to play continuous and intact music sheet with complicated inter-finger movements. Second, the precision of simulator can be further improved by modelling the hammer strikes and tension of strings for the piano environment. Additionally, the simulator and robot platform to perform planning and optimization of the wrist motion and the stiffness of the hand to enable more expressive piano playing.

#### ACKNOWLEDGMENT

This work was supported by the EU-funded Marie Skłodowska-Curie SMART project (grant agreement ID 860108).

#### REFERENCES

- [1] A. Lim, T. Ogata, and H. G. Okuno, "Towards expressive musical robots: A cross-modal framework for emotional gesture, voice and music," *EURASIP Journal on Audio, Speech, and Music Processing*, vol. 2012, no. 1, pp. 1–12, 2012.
- [2] J. Solis, K. Ozawa, M. Takeuchi, *et al.*, "Biologically-inspired control architecture for musical performance robots," *International Journal of Advanced Robotic Systems*, vol. 11, no. 10, p. 172, 2014.
- [3] A. Lim, T. Mizumoto, T. Takahashi, T. Ogata, and H. G. Okuno, "Programming by playing and approaches for expressive robot performances," in *IROS Workshop on Robots and Musical Expressions*, 2010.

- [4] S. Sugano and I. Kato, "Wabot-2: Autonomous robot with dexterous finger-arm-finger-arm coordination control in keyboard performance," in *Proceedings. 1987 IEEE International Conference on Robotics and Automation*, IEEE, vol. 4, 1987, pp. 90–97.
- [5] D. Zhang, J. Lei, B. Li, D. Lau, and C. Cameron, "Design and analysis of a piano playing robot," in *2009 International Conference on Information and Automation*, IEEE, 2009, pp. 757–761.
- [6] L. Jen-Chang, H.-C. Li, K.-C. Huang, and S.-W. Lin, "Design of piano-playing robotic hand," *IAES International Journal of Robotics and Automation*, vol. 3, no. 2, p. 118, 2014.
- [7] Y.-F. Li and C.-Y. Lai, "Intelligent algorithm for music playing robot—applied to the anthropomorphic piano robot control," in *2014 IEEE 23rd International Symposium on Industrial Electronics (ISIE)*, IEEE, 2014, pp. 1538–1543.
- [8] L. Scimeca, C. Ng, and F. Iida, "Gaussian process inference modelling of dynamic robot control for expressive piano playing," *Plos One*, vol. 15, no. 8, 2020.
- [9] A. Topper, T. Maloney, S. Barton, and X. Kong, "Piano-playing robotic arm," 2019.
- [10] J. Hughes, P. Maiolino, and F. Iida, "An anthropomorphic soft skeleton hand exploiting conditional models for piano playing," *Science Robotics*, vol. 3, no. 25, 2018.
- [11] Y. Wei, Y. Chen, T. Ren, *et al.*, "A novel, variable stiffness robotic gripper based on integrated soft actuating and particle jamming," *Soft Robotics*, vol. 3, no. 3, pp. 134–143, 2016.
- [12] K. Mizushima, T. Oku, Y. Suzuki, T. Tsuji, and T. Watanabe, "Multi-fingered robotic hand based on hybrid mechanism of tendon-driven and jamming transition," in *2018 IEEE International Conference on Soft Robotics (RoboSoft)*, IEEE, 2018, pp. 376–381.
- [13] K. Gilday, J. Hughes, and F. Iida, "Jamming joints for stiffness and posture control with an anthropomorphic hand," in *2021 IEEE 4th International Conference on Soft Robotics (RoboSoft)*, IEEE, 2021, pp. 134–140.
- [14] J. Zhou, Y. Chen, Y. Hu, *et al.*, "Adaptive variable stiffness particle phalange for robust and durable robotic grasping," *Soft robotics*, vol. 7, no. 6, pp. 743–757, 2020.
- [15] Y. Yang, Y. Zhang, Z. Kan, J. Zeng, and M. Y. Wang, "Hybrid jamming for bioinspired soft robotic fingers," *Soft robotics*, vol. 7, no. 3, pp. 292–308, 2020.
- [16] H. Xu, Y. Luo, S. Wang, T. Darrell, and R. Calandra, "Towards learning to play piano with dexterous hands and touch," *arXiv preprint arXiv:2106.02040*, 2021.
- [17] G. E. Broman, M. Trotter, R. R. Peterson, *et al.*, "The density of selected bones of the human skeleton," *American Journal of Physical Anthropology*, vol. 16, pp. 197–211, 1958.